The SALT HRS spectrograph: instrument integration and laboratory test results

D. G. Bramall[a], J. Schmoll[a], L. M. G. Tyas[a], P. Clark[a], E. Younger[a], R. M. Sharples[a], N. A. Dipper[a], S. G. Ryan[b], D. A. H. Buckley[c], J. Brink[c]
[a] Centre for Advanced Instrumentation, Durham University, U.K.
[b] School of Physics, Astronomy and Mathematics, University of Hertfordshire, U.K.
[c] Southern African Large Telescope, South African Astronomical Observatory, South Africa

ABSTRACT

SALT HRS is a fibre-fed, high dispersion échelle spectrograph currently being constructed for the Southern African Large Telescope (SALT). In this paper we highlight the performance of key optical components, describe the integration tasks that have taken place and present some first light results from the laboratory. The instrument construction is well advanced and we report on the attainment of the required mechanical and thermal stability and provide a measurement of the input optics performance (including the fibre feed). The initial optical alignment of both the fibre input optics, including image slicers, and the spectrograph optics has taken place and is described.

Keywords: Spectrograph, échelle, SALT

1. INTRODUCTION

SALT HRS is a dual beam, white pupil design that will generate stable, high-resolution spectra for a single object and a sky sample. Wavelength coverage is from 370nm to 890nm in two bands with the crossover point at 555nm. The instrument has four modes of operation: low (LR), medium (MR) and high (HR) resolution (R ~ 16,500, 32,000 & 65,000 respectively) plus a high stability (HS) mode which is a duplicate of the HR mode but with superior fibre scrambling and the option of either superimposing iodine absorption lines or interlacing ThAr spectra for improving the long-term spectral stability. The LR and MR modes are fed by 500μm core fibres and the HR an HS by a smaller, 350μm core fibres. The MR and HR/HS modes include image slicers to re-format the fibre image as a narrow slit. The LR mode has no such imager slicers but by virtue of the wider order separation produced is capable of nod and shuffle [1] for better sky subtraction. A summary of the features available in each mode is given in Table 1.

	LR	MR	HR	HS
Fibre core (μm)	500	500	350	350
Resolving power	16,500	32,000	65,000	65,000
Image slicers	N	Bowen-Walraven	Bowen-Walraven	Bowen-Walraven
Mode scrambling	N	N	N	Y
Nod & Shuffle	Y	N	N	N
Iodine cell	N	N	N	Optional
Simultaneous ThAr	N	N	N	Optional

Table 1 Available spectrograph modes

1.1 Review of Instrument Design

The original optical concept for the spectrograph was prepared by S. Barnes [2] and is shown in Figure 1. Only the blue arm is shown – the red arm is a mirror image of the blue one from the dichroic onwards. It is a white pupil design with an R4 échelle grating which is illuminated by a 200mm beam. The spectrograph footprint is roughly 4m x 1m. The dispersed light from the grating is spilt into the two bands using a dichroic mirror at 555nm (with a spectral gap smaller than 10nm at the crossover). Light in each arm is then cross dispersed by a volume phase holographic grating before it is focused onto the detector by a fully dioptric camera. The spectrograph is fed using a fore optics arm which transforms the f/3.8 ratio at the fibre exit to f/25 through the image slicers and then back again to f/10 to feed the collimator. The fibre input optics, including the image slicers, for each mode are in permanent alignment and a cam driven mask (located

Ground-based and Airborne Instrumentation for Astronomy IV, edited by Ian S. McLean, Suzanne K. Ramsay, Hideki Takami, Proc. of SPIE Vol. 8446, 84460A · © 2012 SPIE · CCC code: 0277-786X/12/$18 · doi: 10.1117/12.925935

directly in front of the slits) blocks light from all but the currently selected mode. The trade-offs which took place to optimise the instrument performance at the point when the key optical components were specified for manufacture were discussed in a previous paper [3]. SALT HRS is expected to deliver the performance outlined in Table 2.

Criteria	Nominal performance
Wavelength range	370-890nm (2 bands)
Spectral resolution	R ~ 16, 500, 32, 000, 65,000
Overall efficiency	HR/MR >10% at 480 and 650nm LR > 20% at 480 and 650nm (excluding telescope & input losses)
Spectral Stability	<0.1 pixel over 3 hrs
Quick-look data reduction	Extracted wavelength-calibrated spectra within <3 minutes
Exposure meter	S/N>10 for V<13 magnitude

Table 2 Key performance criteria

1.2 Instrument Stability

For the highest radial velocity precision the instrument should achieve a temperature stability approaching 1mK. To this end the entire spectrograph is enclosed inside a heated vacuum chamber to provide immunity from refractive index variations in the light path and maintain close control over the instrument temperature. The vacuum vessel is further encased in an insulating jacket and is sited in an enclosure which is maintained at temperature of 22°C ± 0.5°C by a closed loop air conditioner which provides immunity from temperature fluctuations in the spectrograph room and eliminates seasonal variations.

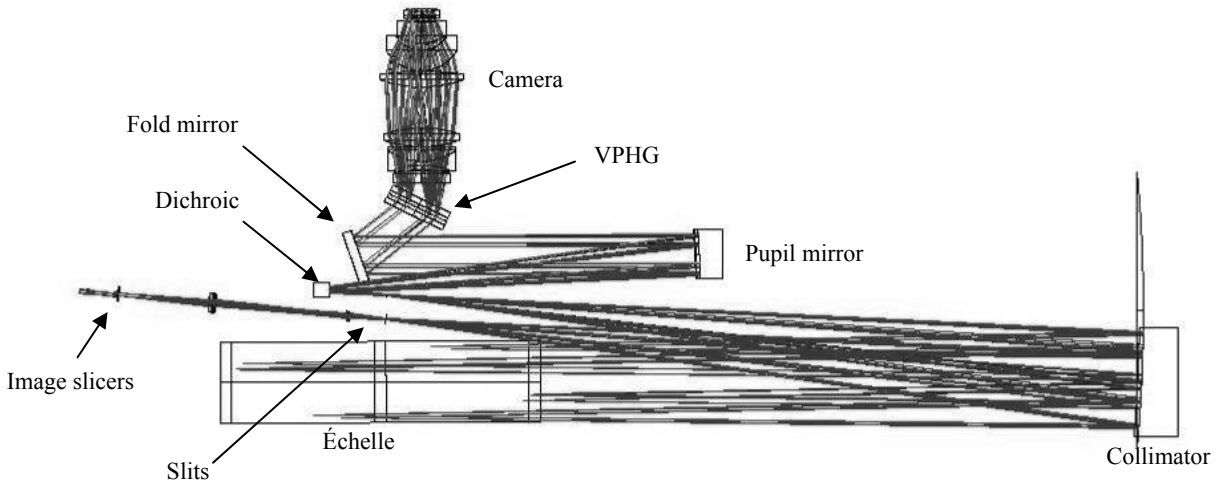

Figure 1 Optical layout (blue arm only is shown). The dichroic is positioned at the fold in the light path centre-left of the diagram.

2. COMPONENT PERFORMANCE

2.1 The Échelle Grating

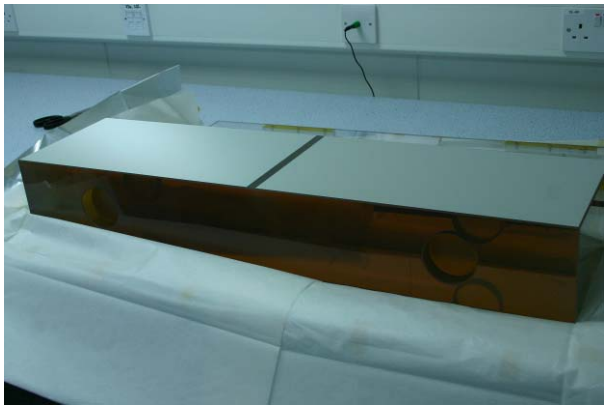

Figure 2 The échelle grating during delivery inspection

The échelle grating is a double replica of a 41.59 groove/mm grating with a 76° blaze angle that has been reproduced on a Zerodur substrate by Richardson Gratings. The grating was optically tested after replication and the results are summarized in Table 3.

Parameter	Measurement
Spectral resolution	736,000 at 632.8nm
Spatial resolution	~0.3 arc sec
Ghost intensity	$< 4.0 \times 10^{-5}$ (relative to parent)
Blaze angle	76.2°
Efficiency (un-polarised, average S&P plane)	> 67% at 360nm > 65% at 400nm > 63% at 550nm > 62% near 900nm

Table 3 Summary of measured échelle characteristics

2.2 Mirrors

The large mirrors were all figured in Zerodur by KiwiStar Optics. The collimator is an off-axis parabolic mirror with a footprint of approximately 600 x 70mm. It is sourced from a 735mm f/2.7 on-axis parabolic parent having a focal length of 2000mm. It has a custom reflective coating optimised for the very broad 380-890nm range. The two pupil mirrors are on-axis concave, spherical mirrors with a footprint of 450x150mm and are identical except for the wavelength optimised coating in the red and blue channels. The pupil mirrors reduce the size of the pupil by a factor of 1.8. The surface form attained on each of the mirrors, along with the achieved coating performance of the collimator, is shown in Table 4.

Parameter	Wavefront error		Coating reflectivity
	PV (nm)	RMS (nm)	
Red pupil mirror	92	20	
Red fold mirror	115	18	
Blue pupil mirror	66	14	
Blue fold mirror	112	23	
Collimator	119	24	84.3% at 380nm 87.8% at 390nm 91.6% at 400nm > 96.2% above 450nm

Table 4 Summary of mirror wavefront errors (all measured at 633nm) and reflectivities

2.3 Dichroic

The blue and red wavelengths are separated by a dichroic with a crossover nominally at 555nm. The blue arm is configured to be in reflection and the red in transmission. The manufactured optic has a transition region that is approximately 20nm wide. It has been decided that to maximise the orders captured at the extreme red end of the spectrum, the dimmest of the overlapping orders will not be imaged on the red CCD.

2.4 Cross dispersers

Cross dispersion is achieved through the use of volume phase holographic gratings. The red and blue gratings have line densities of 855 l/mm and 1850 l/mm respectively. We have measured the first diffracted order transmission efficiency across the entire wavelength range using a monochromator. A comparison with the theoretical efficiencies computed using models is given in Table 5.

	Throughput (%)	
Wavelength (nm)	**Theoretical**	**Measured 1st order**
405	77	72
532	58	55
633	86	82

Table 5 VPHG efficiency

2.5 Cameras

The two cameras were manufactured by SESO (Societe Europeenne de Systemes Opticques, Aix-en-Provence, France). The blue camera assembly comprises 8 lenses and has a clear aperture of 150mm while the red camera has 6 lenses and a clear aperture of 170mm. Both cameras have a cylindrical field flattening lens as the last element which has been made removable such that it can also act as the window for the detector cryostats. The working conditions of the cameras could not be re-created at the supplier as a pre-aberrated source was not available to replicate the spectrograph optics. Instead, the cameras were tested in double pass transmission (at 633nm) with an autocollimating flat mirror across the field of view of the cameras. The wavefront error for the cameras alone (shown in Tables 6 and 7) was found by subtracting the expected aberrations computed in Zemax from the measured performance.

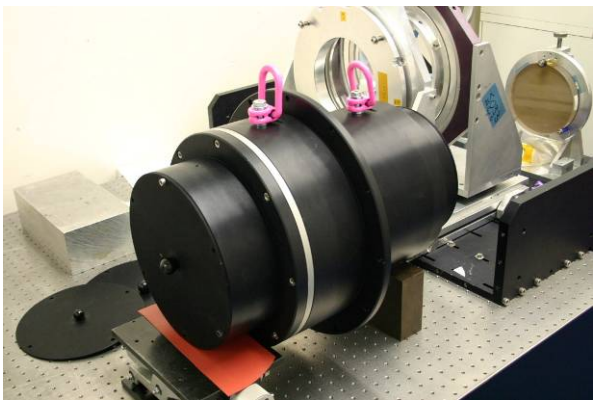

Figure 3 The blue camera acceptance test

Parameter	Measurement
Focal length	199.085mm
WFE (on axis)	0.27λ (λ=633nm)
Global transmission	> 94.5%

Table 6 Summary of red camera tests

Parameter	Measurement
Focal length	166.778mm
WFE (on axis)	0.44λ RMS (λ=633nm)
Global transmission	> 85 % at 380nm > 88.5% at 410nm > 92% above 450 nm

Table 7 Summary of blue camera tests

2.6 Detectors

The blue arm has an e2v CCD 44-82 blue detector which is thinned and back illuminated. It has a broadband anti-reflective coating aplpied. The pixel format is 2048 x 4096 (15µm pixels) and can be read out using one or two readout registers at speeds up to 1MHz. The software also features optional pre-binning and up to 5 readout windows may be specified. The red CCD is a 4096 x 4096 e2v 231-84, again with 15µm pixels. This chip is manufactured from deep depletion silicon and has the Extra Red Plus fringe suppression option. The fringe suppression process attenuates the internal interference fringes seen at long wavelengths (>800nm) on thinned, backside illuminated CCDs. The CCDs are read out using Gen III controllers from Astronomical Research Cameras Inc. These also provide the stabilisation of CCD temperature using a small resistive heater near the chip. The quantum efficiency of the red CCD is 93.1% at 650nm, falling to 58.4% at 900nm.

Port/Speed	890kHz	480kHz	101kHz
Lower left	4.52e-	3.56e-	2.87e-
Lower right	4.45e-	3.41e-	2.82e-
Upper right	4.72e-	3.60e-	2.95e-
Upper left	5.13e-	3.88e-	2.95e-

Table 8 Red CCD read noise

Port/Speed	1MHz	400kHz	100kHz
Left	5.79e-	4.13e-	3.80e-
Right	5.86e-	4.29e-	3.63e-

Table 9 Blue CCD read noise

The detectors are mounted in identical cryostats, which sit outside of the main vacuum chamber and are cooled using closed cycle coolers. Additional work has taken place to maximise the time that the dewar can remain cold before re-pumping is required and, in the case of the red system, the sealing faces have all been re-machined and polished. During its re-assembly best practice in cryostat preparation [4] was followed.

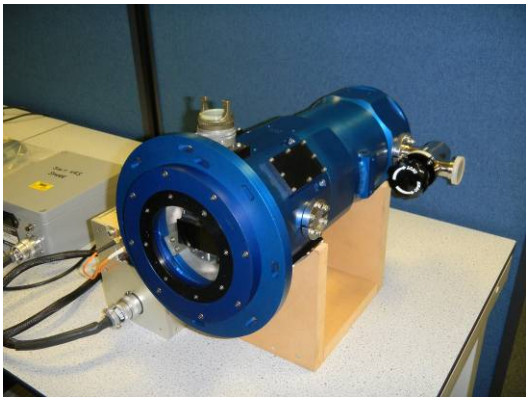

Figure 4 The blue detector dewar

During supplier testing of the HRS blue detector system, contamination unfortunately became deposited on the E2V CCD44-82 active surface. Initial attempts to remove the deposits using alcohol and a single hair brush were only partially successful: a film of residual contamination was still visible on the surface when viewed under a microscope. A second, more aggressive cleaning using ultra-pure (analytical grade) ethanol applied using strips of lens tissue was attempted and has eliminated the marks that were visible in the flat field images. After cleaning the CCD the quantum efficiency of the detector was measured. Given the large experimental error estimates (including additional reflection losses at the dewar window and in extrapolating the photodiode calibration below 400nm) the result was close enough to the manufacturer's data (Figure 5) to conclude that the cleaning of the CCD has not impacted the coating in any way.

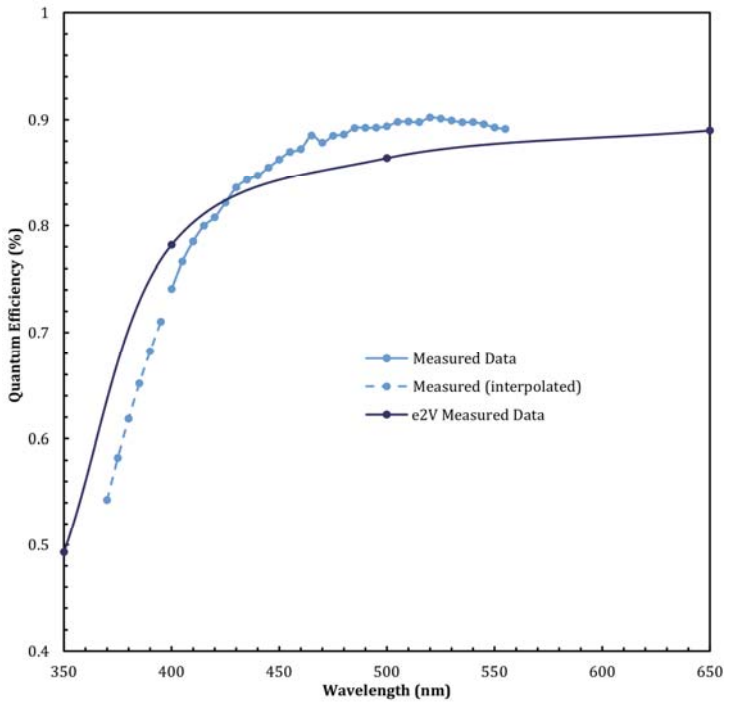

Figure 5 QE for the blue CCD before/after cleaning

2.7 As-built Throughput Model

The most recent throughput predictions for the red and blue arms have been calculated based on the latest available data such as reflectivity measurement of witness samples for coatings and measured CCD quantum efficiency. The throughput estimate includes an actual measurement of the fibre and input optics losses, which are still subject to final optimisations. An independent measurement of the 1st diffracted order transmission efficiency of the VPHGs has been

used (as-built efficiencies were only around 5% worse than the theoretical value). Predictions for the HR and HS sliced modes and the LR mode are shown in Figure 6. The extreme blue performance is restricted mainly by the attenuation of the optical fibres and the reduction in mirror coating reflectivity. It is the VPHG efficiency peaks which give rise to the characteristic bell shape of the efficiencies for each arm. The red arm has higher throughput than the blue due to the increased quantum efficiency of the detector. The LR mode is predicted to have an efficiency in the region of 70% (at 532nm).

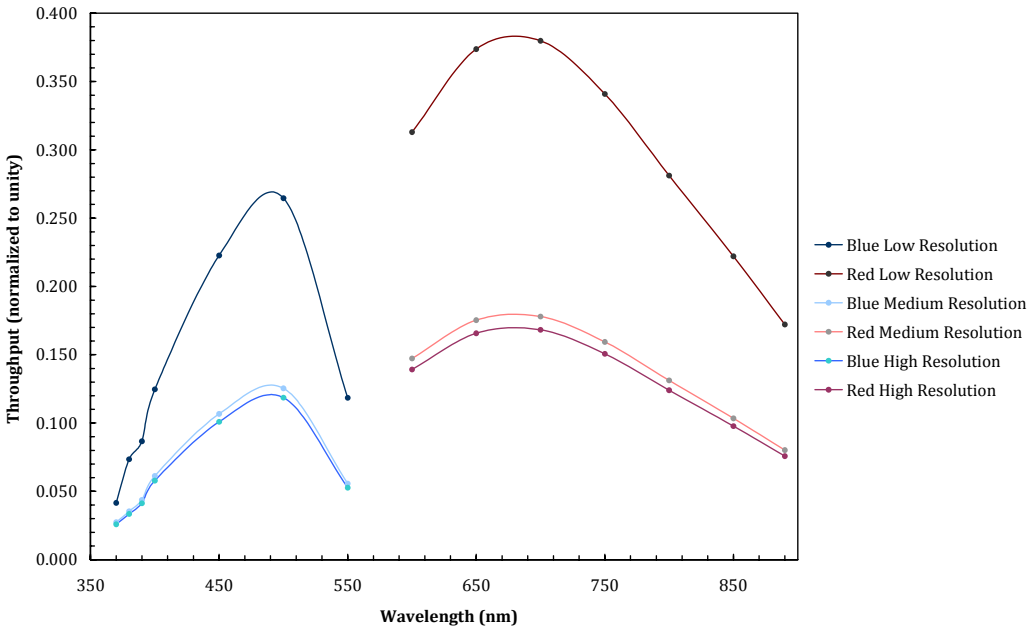

Figure 6. Throughput predictions based on measured performance of individual optics

3. CONSTRUCTION

3.1 Fibre Feed

The fibres are carried from the prime focus of the SALT telescope to the spectrograph room below the telescope pier in a ruggedised conduit. To ensure they are adequately protected, the multi-core fibre protection scheme proposed by Murray *et al.* for the FMOS spectrograph [5] has been followed. Essentially, the fibre cable consists of a central tensile element around which a set of bespoke optical fibre protection tubes are helically wound using the apparatus shown in Figure 7. These tubes are designed to restrict fibre bending and have a high resistance to crushing. To protect the cable from the observatory environment, the wound cable is then sheathed in an outer flexible steel conduit. In this case, four optical fibres (object and sky for each mode plus two spares) were inserted in each protective tube prior to winding. To pack the protection tubes around the central tensile element a fifth (empty) tube was used. This was packed into a conduit with an outer diameter of 25mm. The total length of cable, including a sensible allowance for installation, is 50m. Based on manufacturer's data this implies that the fibre run will have a 90% transmission at 550nm.

Figure 7 Helical winding apparatus (adapted from FMOS)

3.1.1 Fore Optics Alignment

The fore optics alignment, including the placement of all six image slicers has been completed. The slicer alignment was done in-situ once the fibres and their exit lenses had been fixed in place. Shimming of the fibre was required to get all six slicer outputs telecentric while maximising the amount of fibre end surface being imaged inside the slit envelope. A positioning arm mounted on a micrometer stage (see Figure 8) was used to manipulate the tiny optical components (approximately 5mm x 5mm) whilst a video camera was placed at the focus to observe the slices in real time. Once positioned, the slicers were fixed in place using UV-curing vacuum compatible Norland NOA88 adhesive. Figure 9 shows an image of the slits with the light coming from the slicer fore optics. This image will be used to manufacture a photo-etched mask which will produce neat slits of 416μm and 208μm width.

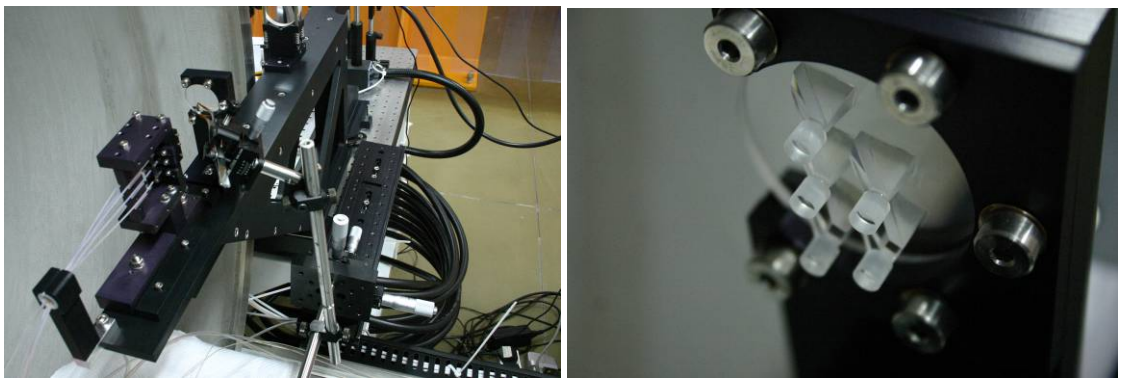

Figure 8 Image slicer manipulation apparatus (left) and close-up of first 5 slicers (right)

Figure 9 Image of the slit plane showing slicer operation – a slit mask will be placed at this location. MR–top, HS–middle and HR-bottom

3.2 Thermal Control

To achieve temperature stability approaching 1mK within the SALT HRS vacuum vessel it is necessary to implement multiple layers of insulation and temperature regulation. An outer enclosure, regulated by an air conditioning unit, controls the ambient temperature to within 0.5˚C. An insulating cover made from plastic coated polystyrene panels will also be constructed around and underneath the instrument to further isolate the vacuum vessel from fluctuations in the outer enclosure temperature. The temperature of the vacuum vessel is actively regulated with a closed loop controller supplying pulses of current to heating wire in direct contact with the vacuum chamber's exterior walls. Pneumatic legs provide isolation from vibration and thermally decouple the instrument from the floor. Figure 10 shows the instrument in its inner thermal enclosure. Also visible is the support frame for the detector dewars and the optical table that holds the

additional optics for the HS mode (namely the iodine cell and ThAr lamp). The fibres enter the vacuum chamber through the two ports on the top of the vessel.

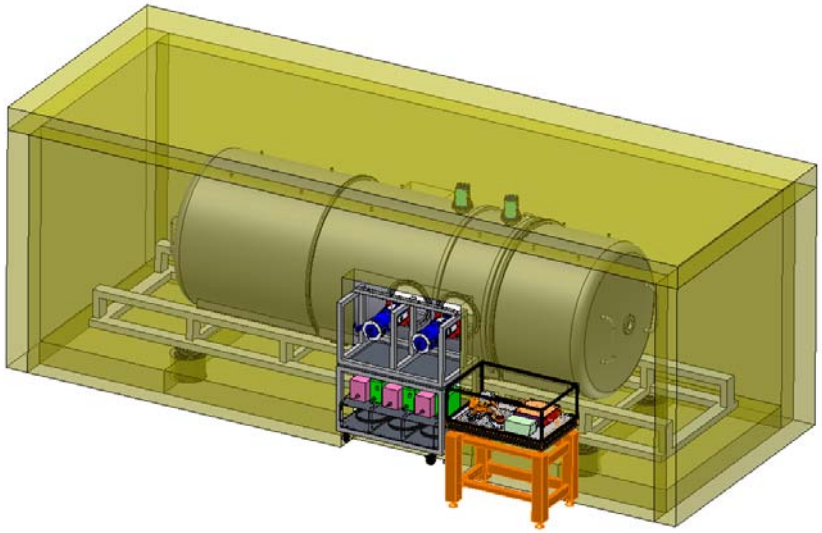

Figure 10 Spectrograph vacuum chamber and inner thermal enclosure.

4. SOFTWARE

4.1 Instrument Control

In line with all SALT instruments, the HRS software will be LabVIEW based and will fully integrate with the state-based scripting concept of the telescope control system. The user interface is written as a client application that is accessible from the telescope operator's console. A single PC runs a control sequence which receives commands from the high level observatory systems and communicates with the low level motion control servers (hosted on the same PC). Image acquisition is performed via two dedicated PCs. A LabVIEW wrapper has been written for the vendor's API to allow the full range of exposure functions, including binning and windowing, to be set through the instrument software. Separate FITS files will be written for the red and blue detector image, complete with headers containing information about the instrument status and observing conditions. These PCs are connected to a data-only network for hiving off the images to the Linux-based data reduction and archiving server. Nod and shuffle operations will be coordinated from the sequencer since both red and blue CCDs must be controlled and commands sent back to the telescope control system.

4.2 Quick Look Data Reduction

The science software to be provided with the instrument will comprise an exposure time calculator and a set of quick look data reduction routines that will each be integrated with the existing SALT tools. The quick look data reduction routines will be based on the FIESTool scripts that were originally developed for the FIES spectrograph at the Nordic Optical Telescope [6]. FIEStool is written in Python and calls specific échelle data reduction routines from external IRAF packages. The basic routines have been reconfigured to run on the blue and red parts of the spectra separately and have been tested using synthetic frames. More advanced reduction tasks such as subtraction of inter-order scattered light, order merging and cosmic ray rejection can also be performed using the software. The data reduction task can be automated once an initial order definition has been made. FIESTool also has scripts to assist in the creation of the master bias and flat field calibration frames that will be required.

The exposure time calculator will implemented in Java. For a particular instrument configuration it calculates estimated exposure times based on instrument throughput, the seeing conditions and a user-provided estimate of the telescope collecting area used for the observation.

5. PLANS FOR COMMISSIONING SCIENCE

5.1 Commissioning Science

SALT HRS was designed to be a flexible instrument capable of a broad range of science. The main science programmes that HRS will undertake are likely to include: stellar radial velocity measurements, stellar atmosphere analysis, chemical compositions of stars, and interstellar and intergalactic absorption. A short, targeted science programme is planned to demonstrate instrument capabilities. For the on-sky commissioning of all four modes of the instrument, the following kinds of observations will be carried out:

- Element abundance measurements of bright, metal deficient standard stars.
- Obtaining spectra from the hosts of short period extra-solar planets to exercise the HS mode with both iodine cell and simultaneous ThAr injection.
- Obtaining spectra from a transiting planet in HR mode with simultaneous ThAr.
- Observing line profile variation of rapidly oscillating Ap type stars in the HR mode.
- Viewing the Lyman alpha forest in spectra of high redshift QSOs in HR mode.
- Obtaining planetary nebulae emission lines from a Magellanic Cloud target in MR mode.
- Viewing of broad absorption lines of QSOs in LR mode with nod and shuffle to test faint object performance.

After commissioning, a full science verification will be undertaken through an open call to the SALT community for demonstration science programmes.

REFERENCES

[1] Glazebrook, K. and Bland-Hawthorn, J., "Microslit Nod-Shuffle Spectroscopy: A Technique for Achieving Very High Densities of Spectra," Publications of the Astronomical Society of the Pacific, 113, 197–214 (2001).

[2] Barnes, S. I. et al, "The optical design of the Southern African Large Telescope High Resolution Spectrograph: SALT HRS," Proc. SPIE, 7014, 70140K, (2008).

[3] Bramall, D. G. et al, "The SALT HRS spectrograph: final design, instrument capabilities and operational modes," Proc. SPIE, 7735, 77354F, (2010).

[4] Deiries, S. et al., "Ultra-clean CCD Cryostats – CCD contamination can be kept under control, Scientific Detectors for Astronomy," Kluwer Academic Publishers, (2004).

[5] Murray, G. J., Dodsworth, G. N., Content, R., "Design and Construction of the Fibre System for FMOS," Proc. SPIE, 7014, 70145L, (2008).

[6] "http://www.not.iac.es/instruments/fies/fiestool/FIEStool.html"